208 *Inorg. Chem.* **2011**, *50*, 208–212
DOI: 10.1021/ic101789u

Inorganic Chemistry
Article

Anionic Gallium-Based Metal−Organic Framework and Its Sorption and Ion-Exchange Properties

Debasis Banerjee,[†] Sun Jin Kim,[‡] Haohan Wu,[§] Wenqian Xu,[⊥] Lauren A. Borkowski,[¶] Jing Li,[§] and John B. Parise*[,†,⊥,¶]

[†]*Department of Chemistry, Stony Brook University, Stony Brook, New York 11794-3400, United States,* [‡]*Nano-Material Research Center, Korea Institute of Science and Technology, P.O. Box. 131, Cheongryang, Seoul 130-650, Korea,* [§]*Department of Chemistry and Chemical Biology, Rutgers University, 610 Taylor Road, Piscataway, New Jersey 08854, United States,* [⊥]*Department of Geosciences, Stony Brook University, Stony Brook, New York 11794-2100, United States, and* [¶]*Mineral Physics Institute, Stony Brook University, Stony Brook, New York 11794-2100, United States*

Received September 1, 2010

A gallium-based metal−organic framework $Ga_6(C_9H_3O_6)_8 \cdot (C_2H_8N)_6(C_3H_7NO)_3(H_2O)_{26}$ [**1**, $Ga_6(1,3,5\text{-BTC})_8 \cdot 6DMA \cdot 3DMF \cdot 26H_2O$], GaMOF-1; BTC = benzenetricarboxylate/trimesic acid and DMA = dimethylamine], with space group $I\bar{4}3d$, a = 19.611(1) Å, and V = 7953.4(6) Å^3, was synthesized using solvothermal techniques and characterized by synchrotron-based X-ray microcrystal diffraction. Compound **1** contains isolated gallium tetrahedra connected by the organic linker (BTC) forming a 3,4-connected anionic porous network. Disordered positively charged ions and solvent molecules are present in the pore, compensating for the negative charge of the framework. These positively charged molecules could be exchanged with alkali-metal ions, as is evident by an ICP-MS study. The H_2 storage capacity of the parent framework is moderate with a H_2 storage capacity of ∼0.5 wt % at 77 K and 1 atm.

1. Introduction

A wide range of metal centers and multifunctional organic ligands are used to construct metal−organic frameworks (MOFs) and coordination polymers (CPs),[1−4] which could be tailored for specific uses such as gas storage,[5−11] ion exchange,[12−14] separation,[15,16] catalysis,[17,18] and sensing and detection.[19−21] One of the advantages of this particular class of materials is that the structural topologies and properties can be tuned by altering synthetic parameters such as the solvent[22−24] and temperature,[25] in addition to the metal ions and organic linkers. Most of the CPs synthesized to date combine aromatic polycarboxylate ligands[26,6] with first-row divalent transition[5−7,27] or trivalent lanthanide[28−30] metal centers, while the use of s- and p-block metal centers is

*To whom correspondence should be addressed. E-mail: john.parise@stonybrook.edu. Phone: (631) 632 8196. Fax: (631) 632 8240.

(1) James, S. L. *Chem. Soc. Rev.* **2003**, *32*, 276–288.
(2) Eddaoudi, M.; Kim, J.; Rosi, N.; Vodak, D.; Wachter, J.; O'Keeffe, M.; Yaghi, O. M. *Science* **2002**, *295*, 469–472.
(3) Cheetham, A. K.; Rao, C. N. R.; Feller, R. K. *Chem. Commun.* **2006**, 4780–4795.
(4) Janiak, C. *Dalton Trans.* **2003**, 2781–2804.
(5) Millward, A. R.; Yaghi, O. M. *J. Am. Chem. Soc.* **2005**, *127*, 17998–17999.
(6) Ma, S. Q.; Zhou, H. C. *J. Am. Chem. Soc.* **2006**, *128*, 11734–11735.
(7) Rowsell, J. L. C.; Millward, A. R.; Park, K. S.; Yaghi, O. M. *J. Am. Chem. Soc.* **2004**, *126*, 5666–5667.
(8) Han, S. S.; Furukawa, H.; Yaghi, O. M.; Goddard, W. A. *J. Am. Chem. Soc.* **2008**, *130*, 11580–11581.
(9) Sun, D. F.; Ma, S. Q.; Ke, Y. X.; Collins, D. J.; Zhou, H. C. *J. Am. Chem. Soc.* **2006**, *128*, 3896–3897.
(10) Dinca, M.; Yu, A. F.; Long, J. R. *J. Am. Chem. Soc.* **2006**, *128*, 8904–8913.
(11) Dinca, M.; Long, J. R. *J. Am. Chem. Soc.* **2005**, *127*, 9376–9377.
(12) Maji, T. K.; Matsuda, R.; Kitagawa, S. *Nat. Mater.* **2007**, *6*, 142–148.
(13) Lin, Z. Z.; Jiang, F. L.; Yuan, D. Q.; Chen, L.; Zhou, Y. F.; Hong, M. C. *Eur. J. Inorg. Chem.* **2005**, 1927–1931.
(14) Fan, J.; Gan, L.; Kawaguchi, H.; Sun, W. Y.; Yu, K. B.; Tang, W. X. *Chem.—Eur. J.* **2003**, *9*, 3965–3973.
(15) Bradshaw, D.; Prior, T. J.; Cussen, E. J.; Claridge, J. B.; Rosseinsky, M. J. *J. Am. Chem. Soc.* **2004**, *126*, 6106–6114.
(16) Kepert, C. J.; Prior, T. J.; Rosseinsky, M. J. *J. Am. Chem. Soc.* **2000**, *122*, 5158–5168.
(17) Wu, C. D.; Hu, A.; Zhang, L.; Lin, W. B. *J. Am. Chem. Soc.* **2005**, *127*, 8940–8941.
(18) Lin, W. B. *J. Solid State Chem.* **2005**, *178*, 2486–2490.
(19) Lu, W. G.; Jiang, L.; Feng, X. L.; Lu, T. B. *Inorg. Chem.* **2009**, *48*, 6997–6999.
(20) Fang, Q. R.; Zhu, G. S.; Xue, M.; Sun, J. Y.; Sun, F. X.; Qiu, S. L. *Inorg. Chem.* **2006**, *45*, 3582–3587.
(21) Lan, A. J.; Li, K. H.; Wu, H. H.; Olson, D. H.; Emge, T. J.; Ki, W.; Hong, M. C.; Li, J. *Angew. Chem., Int. Ed.* **2009**, *48*, 2334–2338.
(22) Chen, S. C.; Zhang, Z. H.; Huang, K. L.; Chen, Q.; He, M. Y.; Cui, A. J.; Li, C.; Liu, Q.; Du, M. *Cryst. Growth Des.* **2008**, *8*, 3437–3445.
(23) Pedireddi, V. R.; Varughese, S. *Inorg. Chem.* **2004**, *43*, 450–457.
(24) Wang, F. K.; Yang, S. Y.; Huang, R. B.; Zheng, L. S.; Batten, S. R. *CrystEngComm* **2008**, *10*, 1211–1215.
(25) Forster, P. M.; Burbank, A. R.; Livage, C.; Ferey, G.; Cheetham, A. K. *Chem. Commun.* **2004**, 368–369.
(26) Park, H.; Britten, J. F.; Mueller, U.; Lee, J.; Li, J.; Parise, J. B. *Chem. Mater.* **2007**, *19*, 1302–1308.

 Published on Web 12/08/2010

comparatively limited. Férey and others have reported a series of trivalent p-block (aluminum-,[31−35] gallium-,[36−42] and indium-based[43−45]) CPs containing interesting architectures and properties. As an example, indium-based networks tend to form anionic porous framework materials with tetrahedrally coordinated indium(III) metal centers.[43,44] A porous anionic framework capable of ion exchange is a potential precursor for inserting alkali-metal cations into the pores.[46] Recently, Hupp et al.[47,48] and Schroder et al.[49,50] have reported being able to "dope" alkali-metal cations in the channels of presynthesized MOFs as a way of increasing the gravimetric storage capacity of the parent materials. The increase in the percentage of H_2 storage is attributed to the high enthalpy of adsorption of gas molecules on the bare metal center. The challenge underlying this strategy is to successfully insert the alkali-metal center into the pore in either metallic or ionic form. The gravimetric advantage of a gallium-based MOF over its indium analogue encouraged us to investigate the formation of coordination networks combining gallium metal centers with different organic linkers under solvothermal conditions. In the course of that investigation, an anionic gallium framework with 3,4 net topology was isolated under solvothermal conditions. In this report, we describe the synthesis, structural characterization, ion exchange, and gas storage studies of Ga_6(1,3,5-BTC)$_8\cdot$ 6DMA$\cdot$3DMF$\cdot$26H_2O (**1**; DMA = dimethylamine) based on isolated gallium tetrahedra and 1,3,5-benzenetricarboxylate (1,3,5-BTC) as the linker.

2. Experimental Section

2.1. Synthesis. Compound **1** was synthesized under solvothermal conditions using Teflon-lined Parr stainless steel autoclaves. The starting materials include gallium nitrate hydrate [$Ga(NO_3)_3\cdot xH_2O$, 99.9%, metal basis, Sigma-Aldrich], 1,3,5-benzenetricarboxylic acid ($C_9H_6O_6$, BTC, 95%, Sigma-Aldrich), ammonium fluoride (NH_4F, 98%, Sigma-Aldrich), *N*,*N*-dimethylformamide (C_3H_7NO, DMF, 99%, Sigma-Aldrich), and ethanol (C_2H_5OH, 99%, Sigma-Aldrich) and were used without any further purification.

Ga_6(1,3,5-BTC)$_8\cdot$6DMA$\cdot$3DMF$\cdot$26H_2O (1). A typical synthesis involves the use of a mixture of 0.001 mol of $Ga(NO_3)_3$ (0.304 g), 0.002 mol of BTC (0.490 g), and 0.001 mol of NH_4F (0.048 g). The mixture was dissolved in 14.9 g of DMF and stirred for 4 h to achieve homogeneity [molar ratio of metal salt: ligand:solvent = 1:2:204]. The resultant solution was heated for 5 days at 180 °C. The product was obtained as a block-shaped microcrystal (yield: 50% based on gallium), recovered by filtration, and subsequently washed with ethanol. Elem anal. Calcd for **1**: C, 36.74; N, 4.14; H, 4.75. Found: C, 36.79; N, 4.08; H, 4.22 (Galbraith Laboratories Inc., Knoxville, TN). IR (ATR): 2954, 1675, 1450, 1396, 1295 cm^{-1}.

2.2. X-ray Crystallography. A suitable crystal of **1** was selected from the bulk and mounted on a glass fiber using epoxy. Reflections for **1** were collected with 0.5° φ scans at ChemMatCars (Sector 15) at the Advanced Photon Source (APS) synchrotron X-ray storage ring (λ = 0.413 28 Å) using a three-circle Bruker D8 diffractometer equipped with an APEXII detector at 100 K. The raw intensity data were analyzed using the *APEXII*[51] suite of software and corrected for absorption using *SADABS*.[52] The structure was solved using direct methods and refined using *SHELXL*.[52] The single gallium atom in the asymmetric unit was located first, followed by the other atoms in the main framework (oxygen and carbon) from the Fourier difference map. All nonhydrogen atoms were refined anisotropically. Hydrogen atoms were placed using geometrical constraints. Contained within the void spaces of the structure of **1** was a combination of highly disordered neutral solvent molecules and charge-compensating countercations. Thus, the *PLATON*/*SQUEEZE*[53] model was applied to remove the contributions of scattering from the disordered species. The chemical formula of **1** was determined using a combination of thermogravimetric analysis (TGA)−differential scanning calorimetry (DSC), elemental analysis, and single-crystal X-ray diffraction (XRD) studies. The crystallographic details of **1** are summarized in Table 1.

Bulk sample identification and confirmation of the phase purity were determined using powder XRD. Data within a range of 5° ≤ 2θ ≤ 40° (step size, 0.02°; counting time, 1 s/step) were collected using a Scintag Pad-X diffractometer equipped with Cu Kα (λ = 1.5405 Å) radiation. Comparison of the observed and calculated powder XRD patterns for **1** with confirmed phase purity (Figure S1 in the Supporting Information). In situ temperature-resolved powder XRD (Figure S6 in the Supporting Information) was performed on a Rigaku Ultima IV diffractometer equipped with a high-speed semiconductor element

(27) Dinca, M.; Dailly, A.; Liu, Y.; Brown, C. M.; Neumann, D. A.; Long, J. R. *J. Am. Chem. Soc.* **2006**, *128*, 16876–16883.
(28) de Lill, D. T.; Cahill, C. L. *Chem. Commun.* **2006**, 4946–4948.
(29) Ghosh, S. K.; Bharadwaj, P. K. *Inorg. Chem.* **2005**, *44*, 3156–3161.
(30) Guo, X. D.; Zhu, G. S.; Li, Z. Y.; Sun, F. X.; Yang, Z. H.; Qiu, S. L. *Chem. Commun.* **2006**, 3172–3174.
(31) Loiseau, T.; Lecroq, L.; Volkringer, C.; Marrot, J.; Ferey, G.; Haouas, M.; Taulelle, F.; Bourrelly, S.; Llewellyn, P. L.; Latroche, M. *J. Am. Chem. Soc.* **2006**, *128*, 10223–10230.
(32) Loiseau, T.; Serre, C.; Huguenard, C.; Fink, G.; Taulelle, F.; Henry, M.; Bataille, T.; Ferey, G. *Chem.—Eur. J.* **2004**, *10*, 1373–1382.
(33) Volkringer, C.; Popov, D.; Loiseau, T.; Guillou, N.; Ferey, G.; Haouas, M.; Taulelle, F.; Mellot-Draznieks, C.; Burghammer, M.; Riekel, C. *Nat. Mater.* **2007**, *6*, 760–764.
(34) Comotti, A.; Bracco, S.; Sozzani, P.; Horike, S.; Matsuda, R.; Chen, J.; Takata, M.; Kubota, Y.; Kitagawa, S. *J. Am. Chem. Soc.* **2008**, *130*, 13664–13672.
(35) Volkringer, C.; Loiseau, T.; Guillou, N.; Ferey, G.; Haouas, M.; Taulelle, F.; Audebrand, N.; Margiolaki, I.; Popov, D.; Burghammer, M.; Riekel, C. *Cryst. Growth Des.* **2009**, *9*, 2927–2936.
(36) Volkringer, C.; Loiseau, T.; Guillou, N.; Ferey, G.; Elkaim, E.; Vimont, A. *Dalton Trans.* **2009**, 2241–2249.
(37) Volkringer, C.; Meddouri, M.; Loiseau, T.; Guillou, N.; Marrot, J.; Ferey, G.; Haouas, M.; Taulelle, F.; Audebrand, N.; Latroche, M. *Inorg. Chem.* **2008**, *47*, 11892–11901.
(38) Volkringer, C.; Loiseau, T.; Ferey, G.; Morais, C. M.; Taulelle, F.; Montouillout, V.; Massiot, D. *Microporous Mesoporous Mater.* **2007**, *105*, 111–117.
(39) Vougo-Zanda, M.; Huang, J.; Anokhina, E.; Wang, X. Q.; Jacobson, A. J. *Inorg. Chem.* **2008**, *47*, 11535–11542.
(40) Mensinger, Z. L.; Zakharov, L. N.; Johnson, D. W. *Inorg. Chem.* **2009**, *48*, 3505–3507.
(41) Loiseau, T.; Muguerra, H.; Haouas, M.; Taulelle, F.; Ferey, G. *Solid State Sci.* **2005**, *7*, 603–609.
(42) Chaplais, G.; Simon-Masseron, A.; Porcher, F.; Lecomte, C.; Bazer-Bachi, D.; Bats, N.; Patarina, J. *Phys. Chem. Chem. Phys.* **2009**, *11*, 5241–5245.
(43) Lin, Z. Z.; Jiang, F. L.; Chen, L.; Yue, C. Y.; Yuan, D. Q.; Lan, A. J.; Hong, M. C. *Cryst. Growth Des.* **2007**, *7*, 1712–1715.
(44) Chen, S. M.; Zhang, J.; Wu, T.; Feng, P. Y.; Bu, X. H. *J. Am. Chem. Soc.* **2009**, *131*, 16027–16029.
(45) Volkringer, C.; Loiseau, T. *Mater. Res. Bull.* **2006**, *41*, 948–954.
(46) Breck, D. W. *Zeolite molecular sieves: structure, chemistry, and use*; R. E. Krieger: Malabar, FL, 1984; p ix, 771 p.
(47) Mulfort, K. L.; Wilson, T. M.; Wasielewski, M. R.; Hupp, J. T. *Langmuir* **2009**, *25*, 503–508.
(48) Mulfort, K. L.; Hupp, J. T. *Inorg. Chem.* **2008**, *47*, 7936–7938.
(49) Yang, S.; Lin, X.; Blake, A. J.; Thomas, K. M.; Hubberstey, P.; Champness, N. R.; Schroder, M. *Chem. Commun.* **2008**, 6108–6110.
(50) Yang, S. H.; Lin, X.; Blake, A. J.; Walker, G. S.; Hubberstey, P.; Champness, N. R.; Schroder, M. *Nat. Chem.* **2009**, *1*, 487–493.
(51) *APEXII*, version 2009.3-0; Bruker AXS, Inc.: Madison, WI, 2009.
(52) Sheldrick, G. M. *Acta Crystallogr., Sect. A: Found. Crystallogr.* **2008**, *64*, 112–122.
(53) Spek, A. L. *PLATON, a multipurpose crystallographic tool*; Utrecht University: Utrecht, The Netherlands, 2001.

one-dimensional detector and a high-temperature furnace. The sample was heated under a flowing N_2 atmosphere with a heating rate of 10 °C/min.

2.3. Thermal Analysis. A combined TGA−DSC experiment for **1** was performed using a Netzsch 449C Jupiter instrument. The sample was heated from room temperature to 750 °C under a N_2 atmosphere with a heating rate of 5 °C/min (Figure S8 in the Supporting Information).

2.4. IR Spectroscopy. The mid-IR reflectance spectra (400−4000 cm^{-1}, 2.5−25 μm) were measured on a Nicolet 6700 FTIR spectrometer equipped with a Smart Orbit diamond, attenuated total reflectance (ATR) accessory. Measurements from 400 to 4000 cm^{-1} were carried out using a KBr beamsplitter and a thermoelectrically cooled deuterated triglycine sulfate (DTGS-TEC) detector with a KBr window (Figure S9 in the Supporting Information)

2.5. Gas Sorption Measurements. All gas sorption experiments were performed on a volumetric gas sorption analyzer (Autosorb-1 MP, Quantachrome Instruments). Liquid nitrogen and liquid argon were used as coolants to achieve cryogenic temperatures (77 and 87 K, respectively). The experiments were conducted using ultra-high-purity H_2, N_2 (99.999%), and CO_2 (99.998%). The N_2 sorption isotherms were collected using a pressure range of 10^{-6}−1 atm at 77 K. The CO_2 sorption isotherm was performed at 273 K, using a pressure range of 10^{-3}−1 atm. The H_2 sorption isotherms were carried out at 77 and 87 K, respectively, with pressures ranging from 10^{-3} to 1 atm. The initial outgassing process for each sample was carried out at 448 K overnight (under vacuum). An outgassed sample (176 mg) was used in the gas sorption measurements with the sample weight recorded before and after outgassing to confirm the removal of guest molecules. The outgassing procedure was repeated on the same sample between experiments for approximately 30 min to 1 h. Pore properties (e.g., pore volume, pore size, and surface area) were analyzed using *Autosorb*, version 1.50, software.

2.6. Ion-Exchange Experiments. Saturated solutions of $LiNO_3$ and $NaNO_3$ in DMF were separately added to the as-synthesized compound **1** (80−90 mg in each vial). The saturated salt solutions were decanted and replaced by a fresh solution every 24 h for 5 days. The ion-exchanged samples were filtered and washed with DMF before being stored under fresh DMF for 3 days. At this time, they were once again filtered and washed prior to being tested for their metal content using ICP techniques (Galbraith Laboratories Inc., Knoxville, TN).

Table 1. Crystallographic Data and Structural Refinement Details of Compound **1**[a]

empirical formula	$C_{12}H_4GaO_8$
fw	345.87
collection temp (K)	77(2)
wavelength (Å)	0.413 28
space group	$I\bar{4}3d$
cryst syst	cubic
a (Å)	19.9611(9)
volume (Å^3)	7953.4(6)
Z	12
calcd density (g/cm^3)	0.867
abs coeff (mm^{-1})	0.223
F(000)	2052
cryst size (mm)	0.11 × 0.12 × 0.03
Θ range of data collection	1.45−15.97
index range	$-23 \le h \le 26$ $-18 \le k \le 26$ $-26 \le l \le 23$
total no. of reflns	40 804
no. of indep reflns	1648 [R(int) = 0.0473]
GOF	1.07
refinement method	full-matrix least squares on F^2
data/restraints/param	1648/0/51
R1 [on F_o^2, $I > 2\sigma(I)$]	0.0263
wR2 [on F_o^2, $I > 2\sigma(I)$]	0.0598

[a] Data based on the *PLATON*/*SQUEEZE*[53] model.

3. Results and Discussion

1 consists of isolated gallium tetrahedra connected by the organic ligands forming an overall three-dimensional network (Figure 1a). The asymmetric unit of **1** consists of one crystallographically independent gallium metal center (Ga1) and one-third of the organic linker including one carboxylate group (Figure 1b). The gallium metal center is present in the distorted tetrahedral coordination environment with an average distance between the gallium center and the carboxylate oxygen atoms (O1 and its symmetry-equivalent positions) of 1.832 Å. The tetrahedral coordination of gallium with carboxylate oxygen atoms is not common. A number of

Table 2. Selected Bond Lengths (Å) and Angles (deg) of **1**[a]

Ga1−O1	1.8317(12)	O1#1−Ga1−O1	103.99(4)
Ga1−O1#1	1.8317(12)	O1−Ga1−O1#2	121.09(8)
Ga1−O1#2	1.8317(13)	O1#1−Ga1−O1#2	103.99(4)
Ga1−O1#3	1.8317(12)	O1#1−Ga1−O1#3	121.09(8)
C1−C2	1.496(2)	O1−C1−C2	114.13(17)
O1−C1	1.310(2)	C3−C2−C1	120.81(17)
O2−C1	1.201(3)	O2−C1−C2	123.01(18)

[a] Symmetry codes: #1, $y - {}^1/_4$, $-x + {}^1/_4$, $-z + {}^7/_4$; #2, $-x + 0$, $-y + {}^1/_2$, $z + 0$; #3, $-y + {}^1/_4$, $x + {}^1/_4$, $-z + {}^7/_4$.

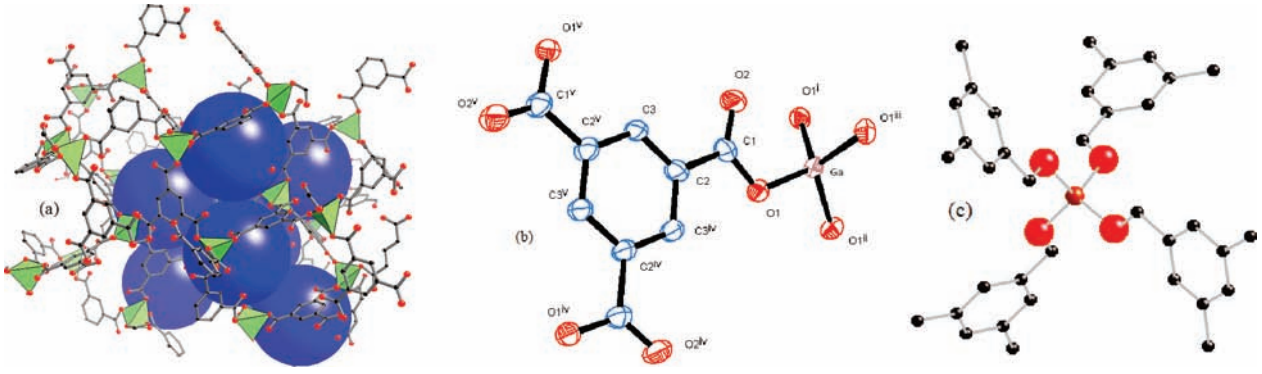

Figure 1. (a) View of **1** from the [111] direction showing the connectivity of the metal ion with the organic linkers. (b) Ellipsoidal plot of the asymmetric unit of **1**. Ellipsoids are shown at the 50% probability level. Hydrogen atoms have been omitted for clarity. Symmetry-related atoms are shown to complete the coordination sphere of the gallium center and organic ligand. Symmetry operators: i (x, y, z), ii ($-x + {}^1/_2$, $-y$, $z + {}^1/_2$), iii ($-x$, $y + {}^1/_2$, $-z + {}^1/_2$), iv ($x + {}^1/_2$, $-y + {}^1/_2$, $-z$), v (z, x, y). (c) Local environment of the gallium metal center in **1**.

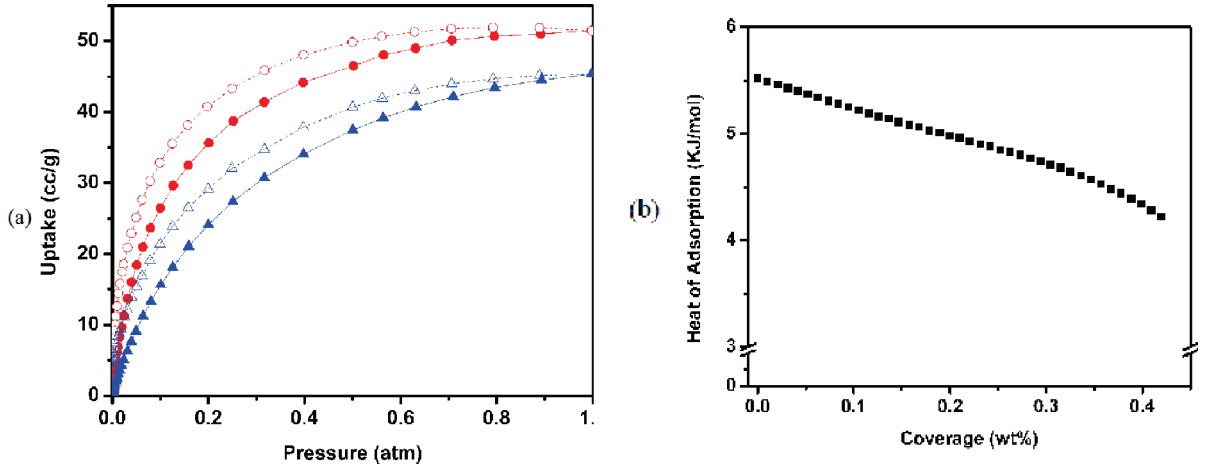

Figure 2. (a) H_2 isotherms at 77 K (red) and 87 K (blue). Adsorption and desorption data are denoted as filled and open symbols, respectively. (b) H_2 heats of adsorption (Q_{st}) calculated based on 77 and 87 K isotherms using the virial method.

tetrahedrally coordinated GaO_4 are reported in the case of open-framework gallium phosphates.[54,55] The coordination number of gallium(III) is strongly influenced by the symmetry, steric requirements, and mode of coordination of the linker. The nature of the solvent and structure-directing agent also plays a major role in the gallium coordination behavior. The bond valence sum[56] of the gallium center is 3.03 valence units, matching well with the expected value of +3.

Each gallium center is connected with four organic linkers (1,3,5-BTC) through their carboxylate oxygen atoms (Figure 1c). Interestingly, only one oxygen (O1) of each carboxylate group participates in a bonding interaction with the gallium metal center. The other oxygen center (O2) remains uncoordinated. The distances between the carboxylate carbon (C1) and the two carboxylate oxygen atoms (O1 and O2) are 1.310(2) and 1.201(3) Å, respectively (Table 2), confirming that O2 remains uncoordinated. Each organic linker is bonded to three gallium centers through each of its carboxylate moieties. Each gallium center is thus connected with eight other gallium centers though four intervening organic linkers. The organic linkers function as the trigonal node while the gallium center is present as the tetrahedral node in the structure, forming a C_3N_4-type 3,4-connected framework. **1** does not have straight channels, although a large void with a diameter of approximately 8 Å is present within the structure. *PLATON*[53] calculates a solvent-accessible volume of 5056.2 $Å^3$ per unit cell, equivalent to a pore volume ratio of 63.57% per unit cell. Disordered counterions and solvent molecules occupy the large void space.

The microcrystalline nature and weak scattering from the sample makes single-crystal XRD data collected on a laboratory-based diffractometer unsuitable for the precise determination of even the framework structure of **1**. While high-quality synchrotron XRD data collected at the APS does allow the precise determination of structural parameters for the framework, characterization of the chemical nature of disordered extra-framework species could not be determined unambiguously from these data alone. The overall formula of **1** can be inferred by considering a combination of the empirical framework formula given in Table 1, the elemental analysis in section 2.1, the analysis of the TGA−DSC results (Figure S8 in the Supporting Information) and IR spectra (Figure S9 in the Supporting Information). TGA−DSC shows an almost continuous weight loss of 37.5 wt % up to 425 °C. We assume that this weight loss is due to extra-framework species alone. The TGA−DSC data thus indicate that the empirical framework formula weight of 345.87 g/mol, calculated based on the single-crystal XRD, accounts for 62.5% of the empirical formula weight of **1**. The empirical formula weight of **1**, including extra-framework species, is calculated to be 553.392 g/mol. The weight percent of C, H, N within the empirical formula was calculated based on the elemental analysis value discussed in section 2.1. The number of formula units in the molecular formula of **1** is determined as 6 because this provides a chemically reasonable charge-balanced formula. The possibility of charge-balancing cations under the synthetic condition of **1** is limited to NH_4^+, H_3O^+, and protonated DMA formed by decomposition of DMF at high temperature and in the presence of water. The possibility of NH_4^+ as a countercation was ruled out in the calculation because the synthesis of **1** can be achieved without the use of NH_4F in the starting reaction mixture. The higher weight percent of nitrogen in the empirical formula derived from the experimental elemental analysis favors the possibility of the presence of positively charged DMA as an extra-framework species. Positively charged DMA probably formed because of decomposition of DMF. On the basis of the above arguments, solvent DMF and water molecules are assigned as the plausible extra-framework species in **1**. IR spectroscopy further confirms the assignment of the extra-framework species. The broad band around 3500−3200 cm^{-1} was assigned for water and DMA for O−H and N−H stretching vibrations, respectively. The presence of a strong band at 1675 cm^{-1} confirms the presence of DMF within the pore. The absence of a strong band around 1700 cm^{-1} shows complete deprotonation of the carboxylic acid groups. Although it was not possible to specifically determine the order of loss of chemical species during TGA−DSC measurements because of the continuous nature of the weight loss, we believe the order to be water > DMF > protonated DMA primarily based on their size and charge. This step is followed by decomposition of the framework between 425 and 540 °C under the experimental conditions. The end product is

(54) Estermann, M.; Mccusker, L. B.; Baerlocher, C.; Merrouche, A.; Kessler, H. *Nature* **1991**, *352*, 320.
(55) Stalder, S. M.; Wilkinson, A. P. *Chem. Mater.* **1997**, *9*, 2168.
(56) Brese, N. E.; O'Keeffe, M. *Acta Crystallogr., Sect. B: Struct. Sci.* **1991**, *47*, 192–197.

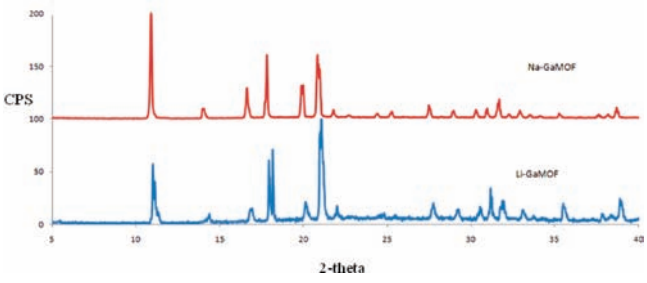

Figure 3. Powder XRD pattern of ion-exchanged compound **1** with alkali-metal cations.

recovered as a black poorly crystalline powder. No further characterization was done on this recovered material.

The sorption properties of **1** were investigated using N_2 and H_2 adsorption isotherms. The Brunauer−Emmett−Teller (BET) and Langmuir surface areas were estimated based on N_2 adsorption isotherms measured at 77 K. The sorption behavior reveals a type I isotherm indicating a microporous material.[57] The BET surface area of **1** based on the N_2 adsorption isotherm is 204.9 m^2/g (Langmuir surface area: 236.2 m^2/g). The pore volume is calculated as 0.11 cm^3/g using the HK method, which uses the N_2 adsorption isotherm.

The H_2 adsorption isotherm for **1** was measured at 77 K. It takes up 0.47 and 0.41 wt % of H_2 at 77 and 87 K, respectively (Figure 2a). The isosteric heats of H_2 adsorption for sample **1** are calculated by the virial method to be between 4.2 and 5.5 kJ/mol in the loading range of 0−0.4 wt % (Figure 2b). It is worth noting that the activation of **1** is strongly dependent on the positively charged cation. The interaction between the positively charged amine cation and the negatively charged framework hinders the complete removal of all extra-framework species. The attempt to remove the positively charged cations by activation either at a higher temperature or for a longer time results in the loss of crystallinity of **1**. Therefore, the adsorption data were collected on samples where the extra-framework counterions were only partially evacuated.

(57) Sing, K. S. W.; Everett, D. H.; Haul, R. A. W.; Moscou, L.; Pierotti, R. A.; Rouquerol, J.; Siemieniewska, T. *Pure Appl. Chem.* **1985**, *57*, 603–619.

The presence of the cationic species within the pore makes **1** a suitable candidate for ion-exchange studies with alkali-metal cations. **1** undergoes partial ion exchange with alkali-metal cations like Li^+ (Ga/Li: 13) and Na^+ (Ga/Na: 6.45), as is evident by ICP studies (Table S7 in the Supporting Information). The powder XRD of an ion-exchanged material shows a pattern similar to that of the as-synthesized compound **1**, indicating that the basic framework remains unchanged upon ion exchange (Figure 3). The TGA−DSC curve of ion-exchange compound **1** showed thermal stability similar to that of the parent compound (Figure S5 in the Supporting Information)

4. Conclusions

A three-dimensional gallium-based anionic framework was synthesized using solvothermal techniques. **1** consists of isolated gallium tetrahedra and 1,3,5-BTC as nodes forming a 3,4-type network encompassing large pores, which contain solvent molecules and counterions. **1** shows a moderate H_2 storage capacity of ∼0.5 wt % at 77 K and 1 atm. It also undergoes partial ion exchange with alkali-metal cations (lithium and sodium), as is evident by ICP-MS studies. Currently, we are exploring similar gallium-based frameworks using different solvothermal conditions.

Acknowledgment. This work is supported by the NSF (Grants DMR-0800415 and DMR-0709069) and NASA (Grant MFRP07-0022). S.J.K. is grateful for support from the Korea Institute of Science and Technology. The authors thank Yu-Sheng Chen (ChemMatCars, APS), Prof. Scott. M. Mclennan, Prof. Timothy. Glotch, and Heidi B. Jensen (Geosciences, Stony Brook) for their assistance during the data collection. ChemMatCars (Sector 15) is principally supported by the National Science Foundation/Department of Energy under Grant CHE-0535644. Use of the APS was supported by the U.S. Department of Energy, Office of Science, Office of Basic Energy Sciences, under Contract DE-AC02-06CH11357.

Supporting Information Available: Figures S1−S9 and a crystallographic information file (CIF). This material is available free of charge via the Internet at http://pubs.acs.org.